Solid-State Electronics 210 (2023) 108789

Contents lists available at ScienceDirect

Solid State Electronics

journal homepage: www.elsevier.com/locate/sse

# Charge dynamics of amino acids fingerprints and the effect of density on FinFET-based Electrolyte-gated sensor

Naveen Kumar [a], César Pascual García [b], Ankit Dixit [a], Ali Rezaei [a], Vihar Georgiev [a,*]

[a] Device Modelling Group, James Watt School of Engineering, University of Glasgow, UK
[b] Nano-Enabled Medicine and Cosmetics Group, Materials Research and Technology Department, Luxembourg Institute of Science and Technology (LIST), Belvaux, Luxembourg

ARTICLE INFO

The review of this paper was arranged by Prof. Sorin Cristoloveanu

ABSTRACT

This work presents the charge dynamics and the effect of the density of amino acids on a sensing surface with the help of analytical modelling. We have implemented an in-house simulator incorporating the Gouy-Chapman-Stern and Site-Binding model to capture the perturbations in the proton affinity of reactive sites with the variation of amino acid density over a sensing surface. The results of the models are explained for Alanine, Glutamic Acid and Histidine with their α-carboxylic terminal immobilized on the sensor surface. The results show that an increase in amino acid density on the sensing surface over a certain limit deviates the fingerprints of the proton affinity away from the affinity of the reactive sites of individual amino acids. The effect of different electrolyte concentrations on steric hindrance is also captured for Alanine and Glutamic Acid. Finally, we used a junctionless FinFET to model unique signatures of amino acids down to a single molecule.

## 1. Introduction

As the building blocks of proteins, amino acids play a crucial role in various biological processes such as building hormones and neurotransmitters, tissue growth or repair, etc. They contain functional groups that can be ionized under specific conditions, leading to changes in their charge state. The charge dynamics of amino acids are affected by various factors, such as temperature, pH and the presence of other ions or molecules. The charge dynamics of amino acids [1] are essential to understand the physicochemical properties and functions of proteins and for studying protein–protein interactions, enzymatic reactions, and other cellular processes. When amino acids are densely packed on the sensing surface, they can experience steric hindrance [2], which can limit the binding of protein ligands to the surface by affecting the ionization of amino acid functional groups, leading to changes in their charge state and properties. A similar effect on the surface energy can happen when a high density of amino acids can lead to increased surface energy. Surface energy is one of the parameters affecting the structural integrity and conformational stability [3] of packed layers of sensor receptors, and it can lead to undesired nonspecific binding of proteins, resulting in a high background signal and reduced specificity of the assay. Understanding the density in surface energy for phenomena like protein folding [4], stability, and function, as well as for designing and optimizing protein-based drugs and therapeutics. In this context, studying the fingerprints of amino acids and their charge dynamics is relevant for developing new technologies and methods for protein analysis and manipulation.

## 2. Methodology

In this study, the analytical model was based on the self-consistent solution of the Gouy-Chapman-Stern (GCS) and Site-Binding model [56]. The calculated surface charge density ($\sigma_o$) using the site-binding model depends on the active surface states ($N_S$), bulk pH ($pH_B$), and dissociation constants ($K_a$ and $K_b$) of the active sites of the amino acids. Each amino acid is immobilized by the α-Carboxylic terminal (C-Imm.) and corresponds to a different $\sigma_o$ due to the active sites (amine site (N) and sidechains) [Alanine (A) ($\sigma_{o1}$), Glutamic Acid (E) ($\sigma_{o2}$), Histidine (H) ($\sigma_{o3}$)] except for the affinity of the C-terminal reacted in the immobilization with APTES [78].

$$\sigma_{o1} = qN_S\left(\frac{cH_S}{cH_S + K_a}\right) \tag{1}$$

* Corresponding author.
*E-mail addresses:* naveen.kumar@glasgow.ac.uk (N. Kumar), cesar.pascual@list.lu (C.P. García), ankit.dixit@glasgow.ac.uk (A. Dixit), ali.rezaei@glasgow.ac.uk (A. Rezaei), vihar.georgiev@glasgow.ac.uk (V. Georgiev).

https://doi.org/10.1016/j.sse.2023.108789

Available online 6 October 2023

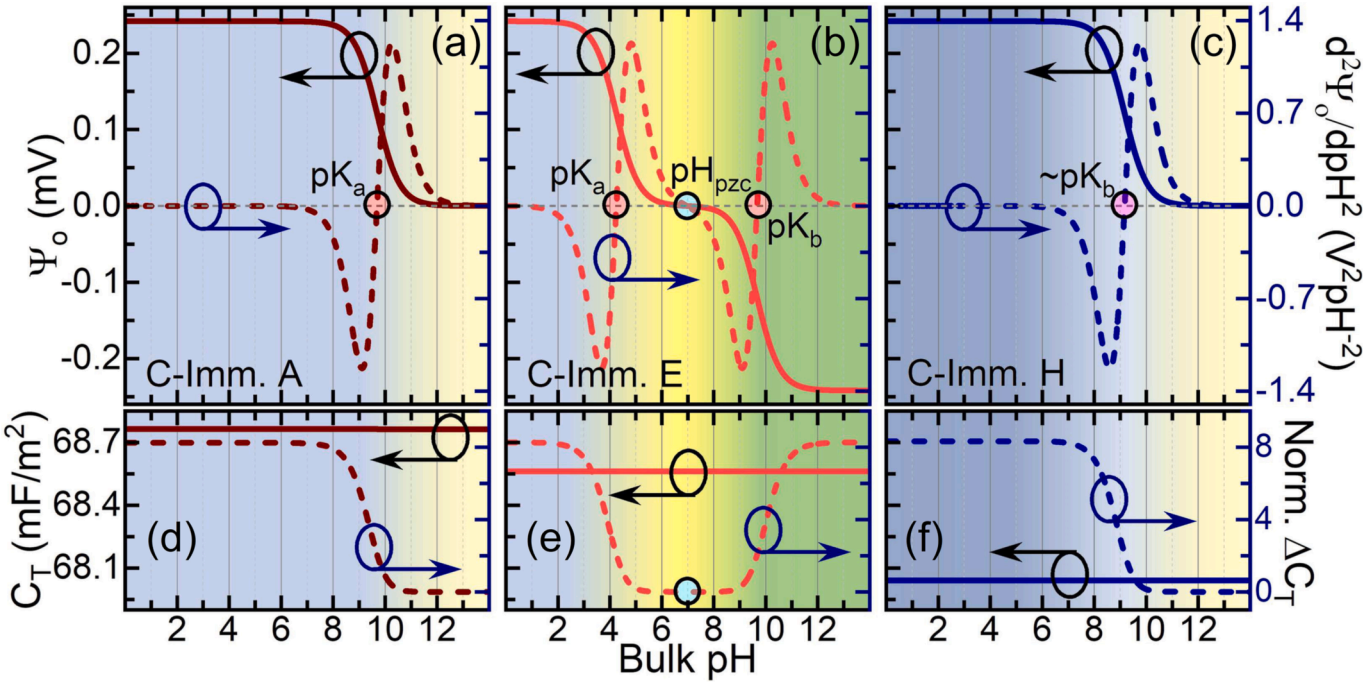


**Fig. 1.** (a) to (c) Surface Potential (solid line) and 2nd Gradient of Surface Potential ($\times 10^{-4}$ $d^2\Psi_o/dpH^2$) (dashed line) for A, E and H amino acids, respectively (d) to (f) Total Capacitance ($C_T$) (solid line) and Normalized $\Delta C_T$ [$\times 10^{-6}$ ($C_T$-min($C_T$))/(min($C_T$))] (dashed line) of ISFET with respect to the pH for Carboxy-terminal immobilized amino acids for A, E and H, respectively. [Note: Calculated for electrolyte concentration = 0.001 M and density = $10^{12}$ mol.cm$^{-2}$].

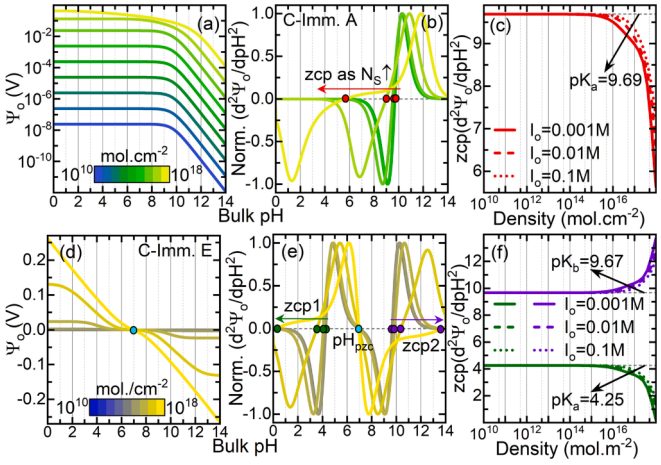


**Fig. 2.** (a) & (d) Surface Potential (b) & (e) Normalized 2nd Gradient of Surface Potential [($d^2\Psi_o/dpH^2$)/(max($d^2\Psi_o/dpH^2$))] of ISFET with respect to the bulk pH for C-Imm. Alanine and Glutamic Acid respectively [Note: Calculated for electrolyte concentration = 0.001 M] (c) & (f) Zero-crossover point (in terms of pH) of $d^2\Psi_o/dpH^2$ of ISFET with respect to the density of C-Imm. Alanine and Glutamic Acid respectively on the sensing surface of Electrolyte-Gated FinFET for different electrolyte concentrations.

$$\sigma_{o2} = qN_S\left(\frac{cH_s^2 - K_aK_b}{cH_S^2 + cH_SK_a + K_aK_b}\right) \tag{2}$$

$$\sigma_{o3} = qN_S\left(\frac{cH_s^2 + cH_SK_a}{cH_S^2 + cH_SK_a + K_aK_b}\right) \tag{3}$$

Where, $(K_a > K_b)$, $cH_s\left(cH_s = cH_B exp\frac{-\Psi_0}{2V_T}\right)$ & $cH_B$ $\left(cH_B = 10^{-pH_B}\right)$ are the surface and bulk proton concentration respectively and $V_T$ is the thermal voltage. Surface potential ($\Psi_o$) is calculated by equating the $\sigma_o$ with the double-layer charge density ($\sigma_{DL}$) from GCS model and the charge density in the semiconducting channel while considering a constant Stern capacitance ($C_{stern}$) of 0.8 Fm$^{-2}$.

## 3. Results and discussion

Fig. 1 shows the output characteristics of the amino acids in terms of $\Psi_o$ (solid line- left y-axis), $d^2\Psi_o/dpH^2$ (dash line- right y-axis) and $C_T$ with respect to the bulk pH. In Fig. 1(a) and 1(b), C-Imm. Alanine and glutamic acid show the variation of $\Psi_o$ from positive to zero and positive to negative respectively as the bulk pH increases from basicity to alkalinity and reflects zero-crossover-point (zcp) of $d^2\Psi_o/dpH^2$ which equals the affinity constant of the corresponding reactive site. At zcp, even with the dynamic process of protonation and deprotonation of reactive sites, the $\sigma_o$ reaches 50% of the value. However, even with two free reactive sites, histidine shows a zcp only for a reactive site with a higher affinity constant due to the similar protonated state of the amine sidechain and α-amine site. The $C_T$ of alanine and histidine decreases with the increase in bulk pH but for glutamic acid, the capacitance shows a U-curve with a minimum at the isoelectric point due to the charged electrical-double-layer capacitance away from the isoelectric point.

The surface potential of C-Imm. alanine decreases for lower densities with a more abrupt transition from the protonated state of the amine site to the deprotonated state as shown in Fig. 2(a). As observed, the zcp of 2nd order differentiation of surface potential shifts towards the lower value (pH) with the increase in the amino acid density. This happens because the diffuse layer thickness decreases for higher densities resulting in an increased $C_T$ allowing the charge to transit state at lower pH due to the electrostatic interaction with the higher concentration of $H^+$ ions (shown by red dots in Fig. 2(b)). As the electrolyte concentration increases, the zcp of 2nd order differentiation of surface potential sustains the decrement towards higher pH values as the higher ionic concentration prevents the charge transition due to interactions with the higher number of counter-ions.

Similarly, for C-Imm. Glutamic acid, the surface potential decreases to lower values as the density decreases throughout the pH range as

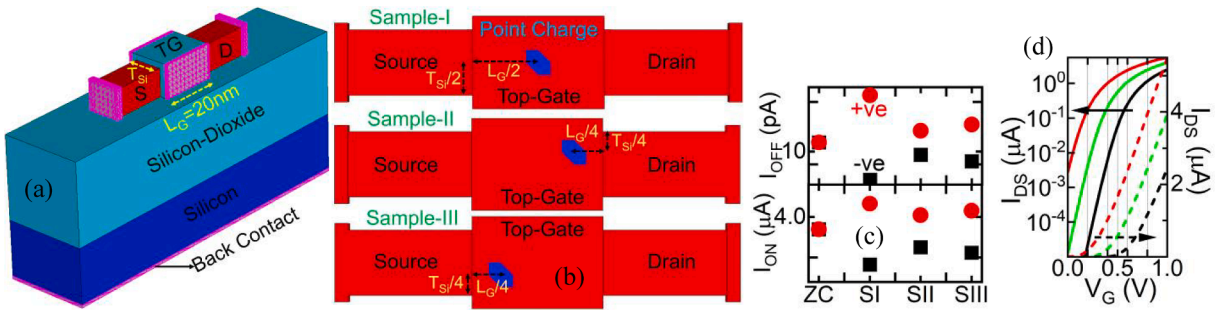


**Fig. 3.** (a) Silicon based n-type SOI-FinFET (b) (I) Sample 1 (SI)- Point charge at the center (II) Sample 2 (SII)- Point charge at the right corner (near drain) (III) Sample 3 (SIII)- Point charge at the left corner (near source) of the top-gate (c) $I_{ON}$ and $I_{OFF}$ for both positive and negative point charges for all three samples (d) $I_{DS}$-$V_{GS}$ characteristics for positive and negative interface charge density of $10^{12}cm^{-2}$. Note: ZC: Zero charge.

shown in Fig. 2(c). The zcp of 2nd order differentiation of surface potential of C-Imm. Glutamic acids confirm the shifting of two zcps (corresponding to the carboxylic sidechain and α-amine reactive sites) away from the isoelectric point which remains the same for all densities. This is due to the higher number of counter-reactive sites (Carboxylic sidechain to amine-reactive site and vice-versa) which balances the charge for a broader range of bulk pH (shown by olive and purple dots in Fig. 2 (e)).

A Silicon-on-Insulator based junctionless Fin-Field-Effect Transistor [9] was simulated using Synopsys TCAD to detect the amino acid based on the observed fingerprints as shown in Fig. 3(a). The gate length of the 10 nm × 10 nm (width × height) FinFET is 20 nm and the doping of source/channel/drain regions is the same as $10^{19}$ $cm^{-3}$ (n-type) respectively. The gate work-function is tweaked to operate the device as npn configuration. Assuming the possibility of single (protonated or deprotonated) amino acid on the sensing surface of the FinFET, a point charge (Fig. 3(b)) and interface charge density was considered in the simulation with positive and negative polarity separately to mimic the conditions. Considering the variability, FinFET was simulated with different locations of a point charge (center, near source and near drain). These data are preliminary data to understand the behaviour of a single point charge, prior to the simulations where we would include the effect of the electrolyte. The device characteristics are analyzed for different samples and compared with FinFET without any charge. The presence of a single protonated amino acid (positive point charge) can change the ON-current ($I_{ON}$) maximum by approx. 0.15μA as compared to approx. 0.18μA for a single deprotonated amino acid (negative point charge) when it is placed at the center of the device. However, for sample-II and sample-III, the variation is limited to approx. 0.09μA. Even for the case of OFF-current ($I_{OFF}$), the device is around 8% more sensitive to positive point charge as compared to its negative counterpart. For the amino acid density of $10^{12}cm^{-2}$ on the sensing surface as interface charge density at extreme (acidic and basic) pH values, a 3-order difference in $I_{OFF}$ and approx. 40% variation $I_{ON}$ is enough to capture the fingerprints of amino acids.

## 4. Conclusions

We have investigated the charge dynamics of the amino acid fingerprints and the effect of higher density on the sensing surface using a developed analytical model. The variability of the affinity constant of amino acids was confirmed at a higher density which can be helpful in accurately predicting the behaviour of amino acids in different biological systems. The simulated FinFET device showed promising results as a platform to detect a single amino acid for a highly sensitive point-of-care sensor or next-generation protein sequencing. The proposed methodology will also help in tackling the non-linearities behind the single-point amino acid sequencing using an Electrolyte-gated FET sensor for the advancement of drug discovery.

## Declaration of competing interest

The authors declare that they have no known competing financial interests or personal relationships that could have appeared to influence the work reported in this paper.

## Data availability

Data will be made available on request.

## Acknowledgments

This project has received funding from the European Union's Horizon 2020 research and innovation program under grant agreement no 862539-Electromed-FET OPEN.

## References

[1] Grånäs O, et al. Femtosecond bond breaking and charge dynamics in ultracharged amino acids. J Chem Phys 2019;151(14):144307.
[2] Yamamoto D, Nakanishi T, Osaka T. Chiral sensing system based on the formation of diastereomeric metal complex on a homocysteine monolayer using field effect transistor. Electrochim Acta 2011;56(26):9652–5.
[3] Ratner BD, Castner DG, Horbett TA, Lenk TJ, Lewis KB, Rapoza RJ. Biomolecules and surfaces. J Vac Sci Technol A 1990;8(3):2306–17.
[4] Nicholls A, Sharp KA, Honig B. Protein folding and association: insights from the interfacial and thermodynamic properties of hydrocarbons. Prot: Struct Funct Bioinformat 1991;11(4):281–96.
[5] Bergveld P, Van Hal REG, Eijkel JCT. The remarkable similarity between the acid-base properties of ISFETs and proteins and the consequences for the design of ISFET biosensors. Biosensors Bioelectron 1995;10(5):405–14.
[6] Dhar R, et al. Deriving a novel methodology for nano-BioFETs and analysing the effect of high-k oxides on the amino-acids sensing application. Solid State Electron 2023;200:108525.
[7] Kumar N, et al. Discovery of amino acid fingerprints transducing their amphoteric signatures by field-effect transistors. ChemRxiv 2022. https://doi.org/10.26434/chemrxiv-2022-bm062-v2.
[8] Kumar N, Dhar R, Garcia CP, Georgiev VP. A novel computational framework for simulations of bio-field effect transistors. ECS Trans 2023;111(1):249.
[9] Shukla RP, Bomer JG, Wijnperle D, Kumar N, Georgiev VP, Singh AC, et al. Planar junctionless field-effect transistor for detecting biomolecular interactions. Sensors 2022;22(15):5783.